PEOPLE'S DEMOCRATIC REPUBLIC OF ALGERIA
MINISTRY OF HIGHER EDUCATION AND SCIENTIFIC RESEARCH
UNIVERSITY OF MOHAMED BOUDIAF - M'SILA

FACULTY OF SCIENCES
Department of Physics
N° : PH/MAT/23/2022

DOMAIN: Sciences of matter
STREAM: Physics
OPTION: Physics of Materials

Dissertation Submitted to the Department of Physics in Partial Fulfillment of the Requirements for the Master's Degree

By: **Kerfal Amani**

Under the title :

Deposition and characterization of undoped and Al doped Zinc Oxide thin films using spray pyrolysis technique

Board of Examiners:

Dr. Fatima Zohra MEZAHI	University of Mohamed Boudiaf - M'sila	Chairperson
Dr. Samir HAMRIT	University of Mohamed Boudiaf - M'sila	Supervisor
Dr. Abdelhafid MAHROUG	University of Mohamed Boudiaf - M'sila	Examiner
Dr. Djamel ALLALI	University of Mohamed Boudiaf - M'sila	Examiner

Academic Year: 2021/2022

Table des matières

Introduction **1**

1 Zinc Oxide: Properties and applications **3**

1.1 Zinc oxide (ZnO): . . . 3

1.1.1 Properties of ZnO: . . . 4

1.1.1.1 Crystal structure of ZnO: . . . 4

1.1.1.2 Optical properties: . . . 5

1.1.1.3 Luminescence properties: . . . 6

1.1.2 Zinc oxide applications . . . 7

1.1.2.1 Cement, Rubber, Paint and Glazes . . . 8

1.1.2.2 Catalysts, Pharmaceutics, Cosmetics and Food Additives 8

1.1.2.3 Gas Sensors . . . 9

1.1.2.4 ZnO as TCO, Solar Cells Applications . . . 9

1.1.2.5 ZnO in ceramic and polymeric membranes for water and wastewater technologies . . . 10

1.1.3 Visions of Future Applications . . . 10

1.1.3.1 pn Junctions . . . 10

1.1.3.2 Light Emitting Diodes . . . 11

1.1.3.3 Field Emitters . . . 11

1.1.4 The doped ZnO . . . 12

2 Deposition and caraterization techniques of undoped and Al doped ZnO thin films **13**

2.1 Fabrication of thin films Oxides . . . 13

2.1.1 Spray pyrolysis technique . . . 14
2.1.1.1 Decomposition of Precursor: . . . 17
2.1.1.2 Substrate Preparation: . . . 19
2.2 Thin film preparation . . . 19
2.2.1 Preparation of solution . . . 19
2.2.2 Deposition of thin films . . . 20
2.3 Characterization Techniques : . . . 21
2.3.1 X-ray diffraction analysis: . . . 21
2.3.1.1 Diffractometer of X-rays system: . . . 24
2.3.2 Optical caracteristic: . . . 24
2.3.3 UV-visible spectroscopy . . . 25
2.3.3.1 Device components: . . . 26
2.3.3.2 Device working principle: . . . 26

3 Results and discussion **28**
3.1 Structural characteristics . . . 28
3.1.1 Spray pyrolysis Undoped ZnO thin films . . . 28
3.1.2 Spray pyrolysis of Aliminium doped ZnO thin films . . . 32
3.2 Optical properties . . . 34

Conclusion **38**

Bibliographie **39**

Liste des figures

1.1 Stick and ball' representation of ZnO crystal structures: (a) cubic rock salt, (b) cubic zinc blende, and (c) hexagonal wurtzite. The shaded gray and black spheres denote Zn and O atoms, respectively. 5
1.2 Schematic representation of a wurtzitic ZnO structure having lattice constants a in the basal plane and c in the basal direction; u parameter is expressed as the bond length or the nearest-neighbor distance b divided by c (0.375) in ideal crystal, and α and β (109.47°) in ideal crystal are the bond angles. 6
1.3 Exciton binding energy (free) for III-V and II-VI semiconductors (m_h^*> m_e^*) 7

2.1 Schematic of spray pyrolysis technique.. 14
2.2 Diagram showing the breakup of a liquid jet by high pressure gas. . . . 16
2.3 Schematics of airless device. 17
2.4 (A) Standing surface waves patterns during the ultrasonic atomisation (water, f=50kHz), (B) Mechanism of droplet break-up for the ultrasonic atomisation. 17
2.5 Deposition processes initiated with increasing substrate temperature. . 18
2.6 Schematics of spray pyrolysis droplet modification 18
2.7 Schematics of elmasonic bath 20
2.8 Schematics of spray pyrolysis equipement 21
2.9 Geometry for interference of a wave scattered from two planes separated by a spacing d. 22
2.10 Schematics of X ray equipement 25

2.11 Spectrophotometere uv-visible 27

3.1 Diffractograme of sprayed ZnO thin film. 29
3.2 Diffractograme of ZnO [01-070-2551]. 30
3.3 Diffractograme of sprayed Al doped ZnO thin film. 33
3.4 Transmission spectra of sprayed ZnO thin film. 35
3.5 Transmission spectra of sprayed ZnO thin film. 36
3.6 Transmission spectra of sprayed doped and undoped ZnO thin film. . . 37

Liste des tableaux

1.1 Some basic properties of ZnO [1]. 4

3.1 XRD data and structural parameters of sprayed undoped ZnO thin film. 31
3.2 Lattice parameters, crystallize size (D), macro strain values (<e>) and dislocation density (δ) of sprayed undoped ZnO films. 32
3.3 Interplanar spacing d_{hkl} from XRD, JCPDS data card for corresponding (hkl) planes, percentage of variation of d, and FWHM of Al doped ZnO sprayed films 34
3.4 the lattice parameters 34

Introduction

Nanotechnology is an interdisciplinary field with enormous potential in the fields of clean energy, medicine, astronomy, chemistry, physics, agriculture, nano-electronics, and environmental remediation. It integrates the basic principles of engineering with different areas of science, with results that are becoming indispensable for human life.

In the last twenty years, the attention of researchers is on metal oxide thin films (metal acts as ction and oxygen act as an anion.) as they show a significant difference in its unique electronic, optical, mechanical, magnetic and chemical properties. One of materials that has been in great interest from wide range of technological field associated with nanotechnology is zinc oxide (ZnO) [1, 2]. Due to its wide band gap (3.3 eV) and large exciton binding energy (60 meV), Zinc Oxide (ZnO) has drawn a lot of attention for nanoscale electronic and optoelectronic device applications [3] . It is used in many applications, such as catalyst, gas sensor, filtering materials for ultraviolet light, and also antimicrobial material.
The physical and chemical properties of ZnO nanocrystals can be efficiently tailored by doping of suitable element into the host matrix for a wider range of possible applications. Researchers paid tremendous attention to doping of wide range of elements (Ni, Fe, Mn, Ag, Cu, Cd, Al, La, Ce etc.) in ZnO [4–6] . The selection of dopant element is aimed to improve the properties of ZnO nanostructures for a particular practical application. Doped ZnO with transition metals (Ni, Fe, Co etc.) and rare-earth metals (La, Ce, Nd etc.), present enhanced ferromagnetic behavior at room temperature and gained more interest for fabrication of spintronic devices. The improved luminescence property of ZnO nanomaterials, doped with alkali metals (Li, K, Na etc.) enables them for phosphor applications. Doping of ZnO nanocrystals with suitable transition metals,

rare metals and noble metals has been preferred to modify their optical and electrical properties, ensuring promising applications of ZnO nanostructures for optoelectronic devices [7,9]. These properties can be further enhanced by varying stoichiometric ratio of dopant element in host material.

There are different physical or chemical deposition methods have been used to prepare the ZnO thin films such as sputtering technique [8] , thermal decomposition [10], thermolysis , chemical vapour deposition, sol–gel [11,12,34] , spray pyrolysis [13], precipitation [14] , vapour phase oxidation , thermal vapour transport, condensation , co-precipitation and Solvo/hydro thermal [15].

Chapitre 1

Zinc Oxide: Properties and applications

In this chapter, we will talk about Zinc Oxide material and its characteristics. Also diffrents applications are mentioned in various fields and the possibility of vaccination with other material to improve some of its properties.

1.1 Zinc oxide (ZnO):

Zinc oxide is an inorganic compound with the formula ZnO. It's in the form of a white powder broken to odorless pale yellow insoluble in water, As oxide ZnO is safe in case of fire and is relatively inert in contact with the human body [20]. It is widely used as an additive in many materials and products such as rubbers, plastics, ceramics, glass, cement, paints and batteries. Zinc oxide is found naturally as the mineral zincite (yellow to red coloring) often containing manganese, but it is largely produced synthetically.
Zinc oxide (ZnO) is a direct wide bandgap semiconductor(3,37 ev). It is transparent in the visible and in the near infrared with an exciton binding energy of 60 meV. [21] Table 1.1 summarizes some of the ZnO properties, considering that ZnO has several unique properties, it has been used in a variety of applications such as in light emitting diodes [17], lasers [18] , piezoelectric transducers, varistors, photocatalytic degradation of environmental contaminants [19], solar cells [16], and chemical sensors [22]

TABLE 1.1 – Some basic properties of ZnO [1].

Property	Value
Molecular Mass	81.37 g/mol
Crystal structure	Wurtzite
Density	5.606 g/cm^3
Melting Point	1975°C
Boiling Point	2360°C
Solubility in water	0.16 g/100 mL
Thermal Conductivity	0.6 ; 1-1.2
Energy gap	3.37 eV
Exciton binding energy	60 mV

1.1.1 Properties of ZnO:

1.1.1.1 Crystal structure of ZnO:

Zinc Oxide crystallize in either rocksalt, cubic zinc-blende or hexagonal wurtzite structure where each anion is surrounded by four cations at the corners of a tetrahedron, and vice versa. This tetrahedral coordination is typical of sp^3 covalent bonding, but these materials also have a substantial ionic character. ZnO is a II-VI compound semiconductor whose ionicity resides at the borderline between covalent and ionic semiconductor. The crystal structures shared by ZnO are wurtzite, zinc blende, and rocksalt, as schematically shown in Fig. 1.1. At ambient conditions, the thermodynamically stable phase is wurtzite. The zinc-blende ZnO structure can be stabilized only by growth on cubic substrates, and the rocksalt NaCl structure may be obtained at relatively high pressures.

The wurtzite structure has a hexagonal unit cell with two lattice parameters, a and c, in the ratio of c/a=8/3 =1.633 and belongs to the space group of C_{4v}^6 or $P6_3mc$. A schematic representation of the wurtzitic ZnO structure is shown in Fig. 1.2. The structure is composed of two interpenetrating hexagonal-close-packed (hcp) sublattices, each of which consists of one type of atom displaced with respect to each other along the threefold c-axis by the amount of u =3/8=0.375 in an ideal wurtzite structure in fractional coordinates the u parameter is defined as the length of the bond parallel to the c axis, in units of c. Each sublattice includes four atoms per unit cell and

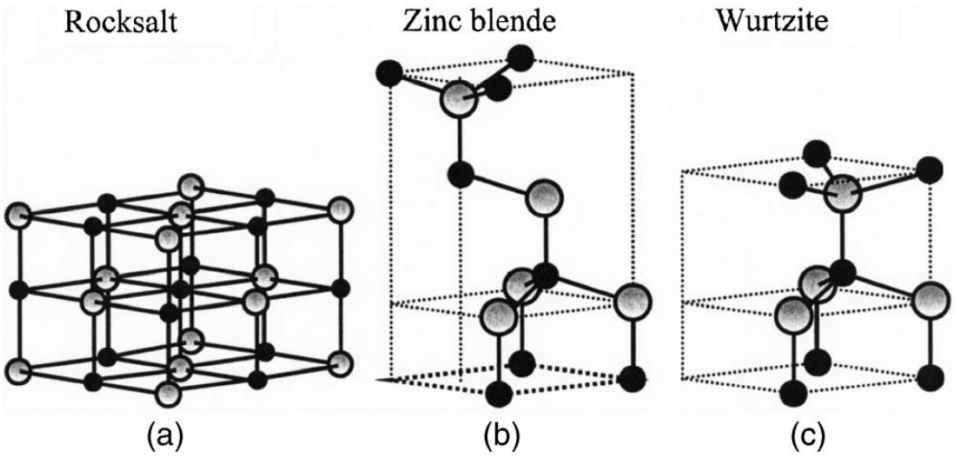

FIGURE 1.1 – Stick and ball' representation of ZnO crystal structures: (a) cubic rock salt, (b) cubic zinc blende, and (c) hexagonal wurtzite. The shaded gray and black spheres denote Zn and O atoms, respectively.

every atom of one kind group-II atom is surrounded by four atoms of the other kind group VI, or vice versa, which are coordinated at the edges of a tetrahedron. In a real ZnO crystal, the wurtzite structure deviates from the ideal arrangement, by changing the c/a ratio or the u value. It should be pointed out that a strong correlation exists between the c/a ratio and the u parameter in that when the c/a ratio decreases, the u param- eter increases in such a way that those four tetrahedral distances remain nearly constant through a distortion of tetrahedral angles due to long-range polar interactions. These two slightly different bond lengths will be equal if the following relation holds:

1.1.1.2 Optical properties:

The interaction of light (electromagnetic wave) with matter (electrons of the material) can clearly explain the optical properties of a material.

The width of the forbidden band is of the order of 3.37eV, greater than that of conventional semiconductors (Table 3.3), this is a fundamental parameter for light emission type applications (diodes and lasers). It is possible to greatly modify the properties of zinc oxide by doping:
Either by deviating from ZnO stoichiometry, mainly by the introduction of atoms of excess zinc in the interstitial position, or by the creation of oxygen vacancies (the

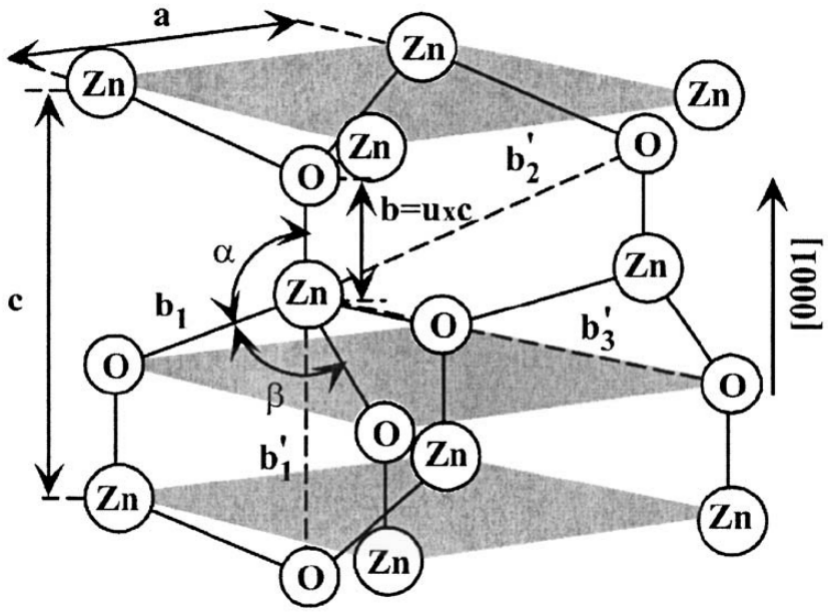

FIGURE 1.2 – Schematic representation of a wurtzitic ZnO structure having lattice constants a in the basal plane and c in the basal direction; u parameter is expressed as the bond length or the nearest-neighbor distance b divided by c (0.375) in ideal crystal, and α and β (109.47°) in ideal crystal are the bond angles.

centers created then behave like electron donors) [24] .
Either by substituting the zinc or oxygen atoms of the network with foreign atoms of different valence (element of group III: F^-, Cl^- for example).

The refractive index (n) is an important parameter when we want to manufacture optoelectronic systems. The structure of ZnO crystal is of compact hexagonal type, which leads to anisotropy of physical properties. In the case of the refractive index, two different indices are obtained depending on the orientation of the crystal, one noted no (polarization E // at the axis c of the crystal) and the other noted ne (polarization E⊥ at the c axis of the crystal). The refractive index of ZnO in the massive form is 2.0 [25] .

1.1.1.3 Luminescence properties:

ZnO is part of the family of transparent semiconductor oxides in the visible domain, which allows it to be classified among the transparent conductive oxides TCO (trans-

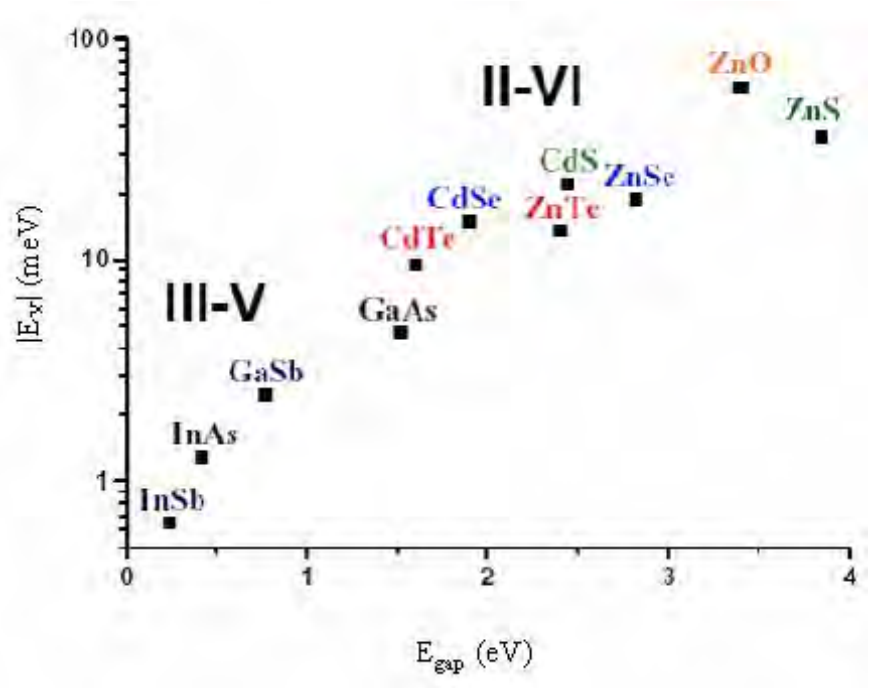

FIGURE 1.3 – Exciton binding energy (free) for III-V and II-VI semiconductors (m_h^*> m_e^*)

parent conductive oxide) when it is doped. It has a strong absorption and diffusion of ultra violet radiation. Zinc oxide is a transparent material with a refractive index of 2 . [26] . Under the action of a high-energy light beam (E> 3.4 eV) or electron bombardment, zinc oxide emits photons.This phenomenon corresponds to luminescence. The Photoluminescence (PL) spectra of ZnO structures have been widely reported.In the near ultra violet and in visible regions, due to its wide band gap charater, ZnO material dispays uminescent properties, (green radiation with a wavelength close to λ = 550 nm). In layers thin, its refractive index and absorption coefficient vary depending on conditions for the development of layers.
Since luminescence is dependent on the doping of the material [27] , this property is used in optoelectronic devices such as cathode ray tube displays, light emitting diodes for color displays, signaling or lighting.

1.1.2 Zinc oxide applications

Among metal oxides, zinc oxide has sparked intensive research efforts to its unique and useful properties in various fields of application Figure.

Historically, ZnO has been used, first for its piezoelectric effect as transducer in wireless radio receivers in the 1920s, before booming considerable in the 1970s in the fields of the chemical industry and pharmaceutical (paint, sunscreens, etc.). Since the 2000s, most of of the global production of zinc oxide, synthesized in nanoscale powder, is used in the rubber and tire industry (57% of the market) as a catalyst in the vulcanization process, chemicals, paints for its protection against UV, agriculture, ceramics and photovoltaic solar cells as a window optical (conductive transparent oxide: OTC).

The catalytic properties of ZnO also give rise to great interest in recent years, particularly in the field of water pollution control. From therefore, ZnO is one of the most promising functional materials due to the technical progress made in terms of synthesis, its intrinsic properties (catalytic, optoelectronic and electrical) and its various morphologies. Among his various fields of application, only the field of photocatalysis is developed in the continuation of this study. [**?**]

1.1.2.1 Cement, Rubber, Paint and Glazes

ZnO serves in large quantities as additive to cement or concrete. It prolongs the cement setting time and improves the hydraulic properties. As an additive to rubber, it improves the rubber cure.Because of its high heat conductivity, it contributes additionally to the transport of heat e.g. out of tires resulting from the crunching.
ZnO is a white pigment used in paints, also known as Chinese white. In contrast to (e.g.) Pb containing pigments, it is not poisonous, does not react with H2Sand does not change its colour under illumination. Partly, TiO2 is replacing it nowadays. Furthermore, ZnO can be added to the glazes of ceramics. [28]

1.1.2.2 Catalysts, Pharmaceutics, Cosmetics and Food Additives

Because of its high absorption over the whole UV spectral range and its good hoto stability, ZnO is used as absorber in sun blockers, but also in other cosmetics and pharmaceuticals. ZnO is known to have anti-inflammatory and bacteriostatic properties. Therefore, it is used in cremes, ointments and on fabrics [29].
It is also found as an additive to human and animal food to compensate Zn deficiencies in nutrition. A nano rod has been used successfully to measure the membrane potential across a human fat cell or the intracellular pH value .

1.1.2.3 Gas Sensors

It is also know n sincemore than half a century that the surface conductivity of ZnO can be strongly modified by the surrounding gas atmosphere, for example by oxygen or hydrogen.These gases are adsorbed to the surface and shift the Fermi levelwith respect to the bands.
In this sense, the action as catalyst is rather directly connected with the sensor application. Some more recent reports on applications of ZnO as gas sensor are given in [30, 31] . One idea is to use ZnO nano rods because of their huge surface-to-volume ratio .Other developments aimat selective coatings of the surface of ZnO, which allow the docking of specific molecules only. This concept can be extended even into the range of ZnO-based biosensors.
Partly as a point of curiosity, it should be mentioned that not only the surface conductivity can be changed by an ambient gas but also the luminescence yield . This effect will also allow an optical reading of such sensors.

Semiconducting metal oxides are one of the most important materials for gas sensors, such as carbon monoxide and hydrocarbons sensors, that are based on variations of the sensor electrical conductance in the presence of those gases. The sensors are typically consisted of a semiconducting oxide film on an insulating substrate, on which two metals are attached as electrodes. A widely used oxide for this appli- cation is tin oxide.

Some of the metal-oxide sensors are humidity-sensitive. The effects of the synthesis parameters on the humidity sensitivity of SnO2-Fe2O3 films have been studied, showing that the utilized iron salt, as the precursor, affects the humidity sensitivity of the SnO2-Fe2O3 films. That is, the films prepared from an alcoholic solution of Fe2(C2O4)3 were more sensitive to humidity than a solution of Fe(NH4)(SO4)2. The ob- servation was discussed based on the higher porosity of the structure prepared from the oxalate precursor as compared to that obtained from the sulfate precursor because several gaseous products are gradually released during the oxalate pyrolysis.

1.1.2.4 ZnO as TCO, Solar Cells Applications

ZnO can be easily n-type doped reaching electron concentrations beyond 1020 cm?3. The doping is generally on the Zn site with Al, Ga or In.. Doping with halides on the anion site is very efficient in other II–VI com pounds like ZnSe but has been less in-

vestigated in ZnO. These highly n-doped samples are essentially transparent in the visible, but bulk, highly Ga-doped samples show a slight bluish colour presumably . These highly dopedwide band gap semiconductors are generally called transpar- ent conducting oxides (TCO).
The ZnO-based TCOs can be produced by many square meters (e.g.) by stuttering. They serve (e.g.) as transparent front contacts for solar cells, liquid crystal displays, in MESFETS or as heat protecting and energy saving coatings for windows, which transmit the visible but reflect the IR. Concerning photovoltaic, early examples of aqueous systems with ZnO electrodes ZnO does not only serve as contact material , but also as a functional one, for example in hybrid solar cells made from n-type ZnO and a p-type semiconductor like Cu2O or from ZnO nano particles and conjugated polymers.
Alternatively, ZnO nano wires can be used in dye sensitized solar cells. In any case, a medium is necessary to extend the absorption spectrum towards longer wavelengths.

1.1.2.5 ZnO in ceramic and polymeric membranes for water and wastewater technologies

- ZnO has been postulated as a filler in polymeric and ceramic membranes
- Recent progress on ZnO nanostructure preparation and characterization is reported.
- Environmental applications using ZnO-embedded polymeric/ceramic membranes are included.
- Approaches to control membrane properties to reduce fouling and biofouling are also covered.

1.1.3 Visions of Future Applications

1.1.3.1 pn Junctions

for ZnO-based semiconductor pn junctions .The n-type region can be easily made from ZnO/X with X D Al, Ga or In. Since first reliable reports on p-type doping have been published recently, ZnO homo junctions have been produced. The other possibility is to grow heterojunctions with n-type ZnO, its alloys or ZnO-based quantum wells and a p-type doped semiconductor such as SiC, Si, GaN, GaAs, NiO,

SrCu2O2,CuCrO2,ZnRh2O4 or even a p-type organic semiconductor. One has to ask, however, in the case of heterojunctionswhy one should use n-type ZnO with p-type GaN, since n-type In1?xGaxN is also readily available.
For LEDs there are both arguments in favour of and drawbacks for heterojunctions . Recently, non-volatile memory devices based on resistance switching including ZnO-based selector elements have been suggested as an application of Schottky or pn junctions . One of themain advantages is said to be the ability to stack these cross-bar memory structures in three dimensions, since there is no need for single crystallinity, such as in silicon. In such a cross-bar memory, a selector element as well as a memory element needs to be realized. As a selector element, a ZnO-based Schottky diode or p-n-diode can be used. For the bit storage element, resistance switching has been demonstrated in another oxide semiconduc- tor,NiO. InNiO, different conduction paths are created after employing high current densities, leading to a reversible resistance switching.

1.1.3.2 Light Emitting Diodes

The most important aspect that drives the present renaissance (or hype) of ZnO research and development (R and D) is the hope to obtain with ZnO a material alternative to or instead of group III-Nitrides for a blue optoelectronics.More specifically, light emitting diodes (LED) or even laser diodes (LD) aremeant fromthe green over
the blue to the near UV spectral range using the combination Zn1-xCdxO=ZnO in the first case and the combinations Zn1-xMgxO=ZnO or Zn1-xBexO=ZnO in the second.

1.1.3.3 Field Emitters

The pointed tips of etched or as-grown, needle-like bulk ZnO crystals enhance the electric field strength if a voltage is applied between the ZnO needle and a counter electrode in vacuum. This fact triggered rather early the idea of field emission from ZnO.
For an early experimental realization. Therefore, it is not surprising that the idea came up again with the availability of nano rods, which have a tip with a small radius of curvature. As a further application-friendly aspect, these nano rods grow in well-defined places on pre-structured substrates. Besides the interest- ing physics and material properties, which can be learned from this effect like the density of surface states, the idea came up to use ZnO nano rods as field emitters in flat panel displays by

accelerating the field emitted electrons onto a phosphor screen. The questions, which have to be answered before a large-scale application becomes possible, concern again the lifetime or degradation of the rods. ZnO is a relatively soft material compared (e.g.) with tungsten, and degradation has been seen even for bulk samples at rather low currents.

1.1.4 The doped ZnO

The properties of ZnO nanocrystals can be efficiently tailored by doping of suitable element into the host matrix for a wider range of possible applications.
Generally, it is possible to dope the matrix of ZnO with metallic elements according to the desired physical properties. We can cite for example:
Al, In, Ga, Mo, Eu, Er, Yb,... for the optoelectronic properties;
Fe, Co, Mn,... for the magnetic properties:

Chapitre 2

Deposition and caraterization techniques of undoped and Al doped ZnO thin films

In this chapter, we present the different elaboration and characterization techniques used in our work. We particularly describe the Spray pyrolysis methode used for the deposition of thin films. And also we discused the characterization thechnique for study the properties of obtained samples including X-rays diffraction (XRD) and UV-Visible spectrophotometry.

2.1 Fabrication of thin films Oxides

There are several deposition techniques have been widely used to produce undoped and doped ZnO thin films. However, seeking the most reliable and economic deposition technique is the main goal. The most intensively studied techniques include, R F magnetron sputtering, chemical vapor deposition (CVD), sol–gel method, thermal evaporation and spray pyrolysis. The chemical bath deposition and sol–gel technique are also well- known methods of preparation of ZnO thin films. Among these, spray pyrolysis is one of the most widely used methods. These new methods range from novel schemes to slight changes to known procedures that provide for the production of a certain desired trait or product.

2.1.1 Spray pyrolysis technique

Spray pyrolysis is a process in which a thin film is deposited by spraying a precursor solution on a heated surface, where the chemical constituents react to form a chemical compound. The chemical reactants are selected such that the products other than the desired compound are volatile at the temperature of deposition. As shown in the (Fig. 2.1), the precursor solution is atomized in a droplet generating apparatus. In spray pyrolysis, the reaction takes place from the vapor phase at moderate high temperature, and can be performed in air for depositing transparent thin films of oxides such as TiO2, ZnO, F-doped SnO2, graphene oxide, etc compact layers on the surface of the transparent conductive. Spray pyrolysis method has been adopted due to its simplicity and relatively cost-effective processing method (especially with regard to equipment cost).

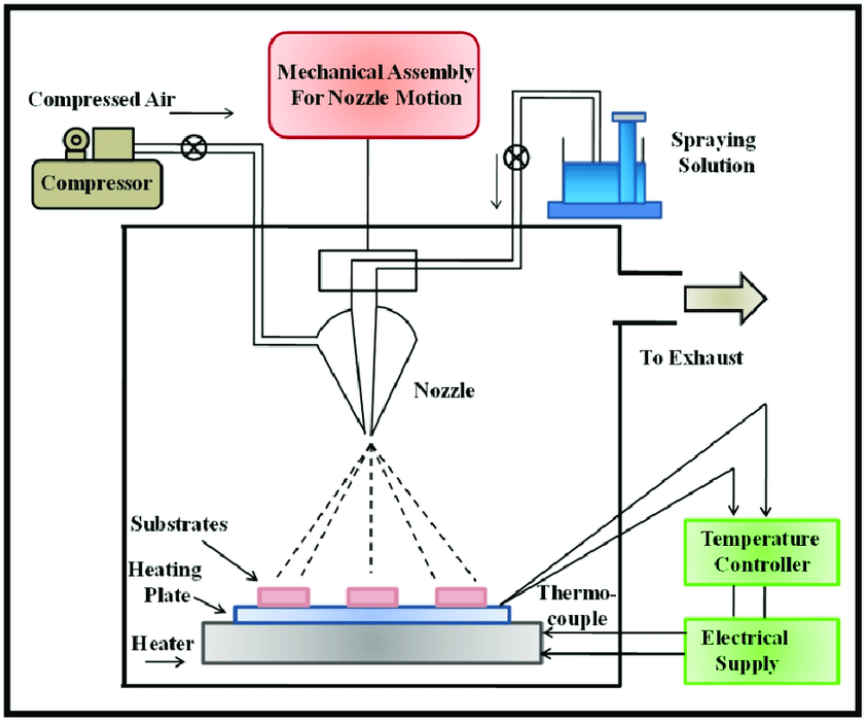

FIGURE 2.1 – Schematic of spray pyrolysis technique..

Due to simplicity of the apparatus and good repeatability of this technique on a large area, it has already become most attractive technique to produce thin films of oxides and sulfides of metals, binary / ternary / quaternary compound semiconductors

and superconducting compounds. In addition to its simplicity spray pyrolysis has a number of advantages; for example it offers an enormously easy way to dope films with any element in any proportion by just diluting the solution we can go even to concentration which cannot be weighed] which help us to change structural, optical and electrical properties.

Typical spray pyrolysis equipment consists of an atomizer, substrate heater, temperature controller and solution container. Additional features of like solution flow rate control, improvement of atomization using electrostatic spray or ultrasonic nebulisation can be incorporated into this basic system to improve the quality of the films. To achieve uniform large area deposition, arrangements for moving either nozzle or substrate or both are used. The schematic diagram of typical spray unit is given below. The atomization of chemical solution into spray of fine droplets is accomplished through spray nozzle with the help of filtered carrier gas.

There are at least four types of spray guns available. They are the pneumatic, the airless, the pneumatic airless, and the ultrasonic.

In the pneumatic system atomization of the solution takes place by the action of compressed air on a fine jet of the spray solution. This jet is broken up by the flow of high pressure gas as shown in Fig.2.2, which forces the liquid out of the atomizer through a narrow orifice.

The second type of spray atomizer is the airless or centrifugal type figure.2.3, where atomization is achieved by forcing the solution directly through a specially designed orifice under high pressure . Using this method the droplets on leaving the atomizer have sufficient velocity to be transported to the substrate without the need for a carrier gas.

The third type of spray atomizer is a combination of (1) and (2). This has the effect of producing a more uniform droplet size.

The fourth type of atomizer is the ultrasonic variety in which a solution is shaken violently as a result of which mists are produced which have a very narrow droplet size distribution.

In spray ultrasonic, a thin liquid film formed on a high-frequency vibrating surface will break-up in a fine uniform spray. The ultrasonic vibration induces surface waves in the liquid film. As frequency is tuned, very regular square cells can be observed on the free surface just before reaching the resonance frequency (Fig. 2.4 (A)). When

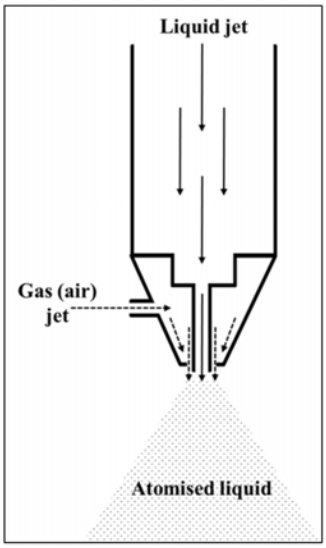

FIGURE 2.2 – Diagram showing the breakup of a liquid jet by high pressure gas.

resonance is reached, the amplitude grows till droplets break-up (Fig. 2.4 (B)). The very regular square cells generate uniform size droplets [5].

SPT is a useful method for the deposition of metal oxides because it is a simple technique with low equipment cost, and requires little maintenance. It does not consume much power compared to vacuum equipment. Also, electricity is not required after using SPT for deposition. The quality and properties of the deposited films depend largely on the process parameters. The substrate surface temperature affects the output of the films. Higher substrate temperatures produce rougher and porous film; but low temperatures give cracked film. Deposition temperature also influences the crystallinity, texture, and other physical properties of deposited film . Precursor solution also affects morphology and properties of deposited film . SPT is grouped into four processes by means of reaction type :

— Process 1: involves the droplet residing on the surface as the solvent evaporates thereby making the solid react when dry.

— Process 2 the solvent evaporates just before the droplet makes contact with the surface. Dry solid impinges on it allowing for decomposition.

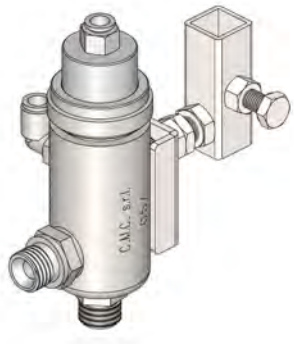

FIGURE 2.3 – Schematics of airless device.

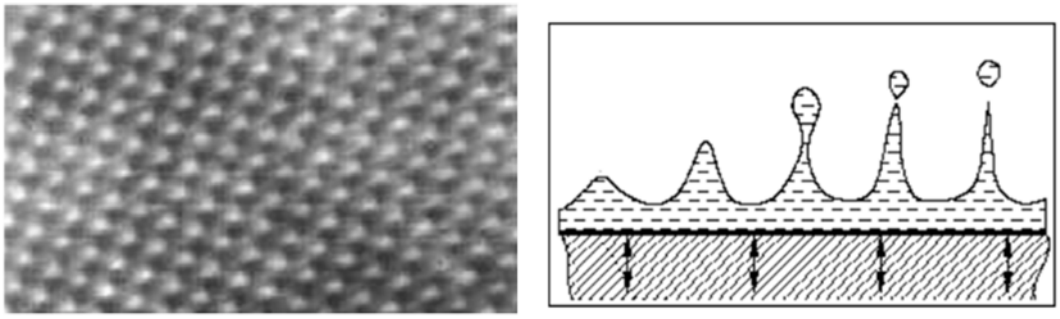

FIGURE 2.4 – (A) Standing surface waves patterns during the ultrasonic atomisation (water, f=50kHz), (B) Mechanism of droplet break-up for the ultrasonic atomisation.

— Process 3 is known as true chemical vapour deposition. Solvent vaporizes as the droplet approaches the substrate. The solid melts and vaporizes. Thereafter, the vapour diffuses to the substrate to undergo heterogeneous reaction.

— Process 4 occurs in the vapour state.

2.1.1.1 Decomposition of Precursor:

Many processes occur simultaneously when a droplet hits the surface of the substrate: evaporation of residual solvent, spreading of the droplet, and salt decomposition. Many models exist for the decomposition of a precursor. This is represented as (A-D) in Figures 2.5 and 2.6. Point (A) is the lowest temperature region. The highest

is D while B and C are in-between A and D.

Processes A and D give rough or non-adherent films. Adherent films are rarely obtained in process C if spray pyrolysis is used. It is caused by low deposition temperature for the precursor vaporization. It can also be caused when the precursor salt decomposes without melting and vaporization.

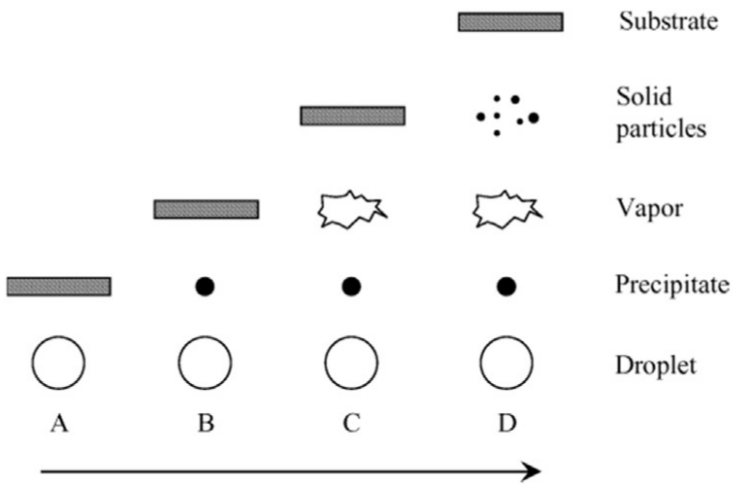

FIGURE 2.5 – Deposition processes initiated with increasing substrate temperature.

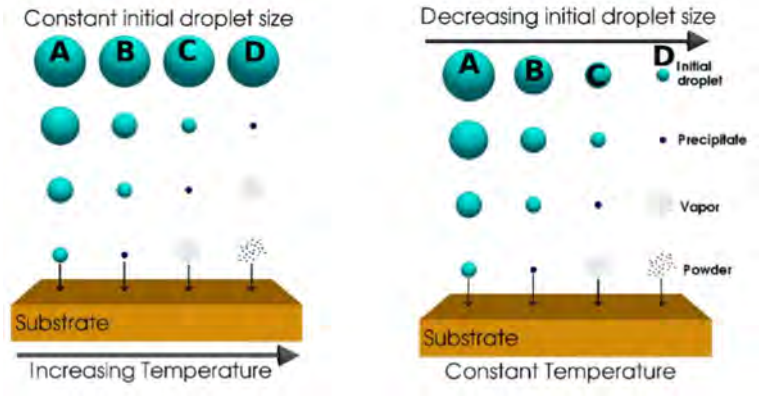

FIGURE 2.6 – Schematics of spray pyrolysis droplet modification

2.1.1.2 Substrate Preparation:

2.1.1.2.1 Substrate chosen The substrate is very important for the growth of thin films in terms of the lattice and thermal mismatching between it and the film because it commonly leads to the development of stress in the deposited film. The choice of substrate affects crystalline quality as well as optical and electrical properties of ZnO film . In this study, The undoped and doped ZnO thin films were deposited in a microscopy slide glass substrates in a size of 2.5x7.5x0.1 cm^3. The choice of glass as substrate was due to three reasons, for economic reasons, to perform a good optical characterization of our films and to minimize the stresses because the two materials constituting the sample (glass + zin oxide) have a very close expension (dilatations) coefficients ($\alpha_{glass} = 8.5\text{x}10^{-6}.K^{-1}$, $\alpha_{zno} = 7.2\text{x}10^{-6}.K^{-1}$)

2.1.1.2.2 Substrate cleaning In thin film technology, clean substrate is an important step prior to deposition. It is necessary to remove the contaminants that would otherwise affect the properties of the films. Cleaning involves the removal of contaminants without damage to the substrate. While cleaning, the bond between the substrates is broken and contaminants are set free from the substrates. The properties that can be affected by the presence of contaminants include morphology, nucleation electronic properties and the substrate film interface.

The substrates were successively sonicated (placed in an elmasonic bath Fig. 2.7) in Acetone, Di-ionized water and ethanol for 10 minutes. Finally they were purged with dryer.

2.2 Thin film preparation

2.2.1 Preparation of solution

Spray aqueous solution was prepared by disolving an amount of $Zn(CH_3COO)_2.2H_2O$ zinc acetate in V volume of alcohol (ethanol and propanol), with stirring magnetic at 40 °C for 20 minutes. Microscopic glass slides, cleaned with organic solvents,were used as substrates. The aqueous solution was sprayed on the substrate by using a seringpump. The spray interruption of 30 seconds was provided after each spray to enhance the migration length of the decomposed ad-atoms of the precursors and also to maintain thermal homogeneity of the substrate. To vary the film thickness the total duration

FIGURE 2.7 – Schematics of elmasonic bath

of the coating was varied. After completion of the deposition process, the films were allowed to cool slowly to room temperature.

2.2.2 Deposition of thin films

Our films were grown using an automated spray system, Holmarc's spray pyrolysis system model HO-TH-04 Company (HOLMARC «OPTO-MECHAT RONICS PVT.LTD» Fig. 2.8, for Laboratory of Materials Physics and its Applications(University of Mohamed Boudiaf Msila), this one has been designed for research laboratories. Parameters like dispensing rate of the n solution and speed of spray head (atomizer) movement are controlled precisely which are difficult to be controlled in manual process. A positive displacement pump controlled by stepper motor and microprocessor is used to dispense solution as per requirement. The spray head movement is also controlled by stepper motor driven linear stages in X and Y direction. The temperature of the substrate heater plate is controlled independently through a dedicated controller. A desk top computer with windows OS is used to control the operations through serial port. This software for spray pyrolysis system can as well be used for documenting the relevant parameters used for sample preparation like temperature, air pressure, duration, etc.

FIGURE 2.8 – Schematics of spray pyrolysis equipement

2.3 Characterization Techniques :

2.3.1 X-ray diffraction analysis:

In 1895, Wilhelm Conrad Roentgen, while working with cathode rays produced by Crookes tubes, discovered the X-ray. After publishing photographic observations of his wife's hand, where the bones could be observed, X-rays were very quickly used to generate medical radiographies and technical applications. However, Ro¨entgen could not evaluate interference, reflection, or refraction effects (Guinebretie're, 2007; Epp, 2016).

Typically, X-ray is an electromagnetic radiation having a wavelength of 1 Å between ultraviolet and gamma rays. In material science, X-rays diffraction is known as a characterization technique capable of investigating the crystalline structures of the grown nanostructures. This non-destructive analytical technique is quite useful for studying chemical composition, crystal structures and their phases, size, symmetry of the unit cell, lattice constants and physical properties of grown materials.

X-ray diffraction characterization is a crucial step in determining the purity and crystallinity of materials after deposition and densification. It's technique based on

the diffraction of X-rays by matter. The general method consists in bombarding the sample with X-rays, and in analyzing the intensity of the X-rays, which is scattered according to the orientation in space. Scattered X-rays interfere with each other, the intensity therefore has maxima in certain directions, we speak of a "diffraction" phenomenon. The intensity detected is recorded as a function of the deflection angle 2θ of the beam. [32]

Fundamental treatment of x-ray diffraction by crystals is done by considering the interaction of an x-ray plane wave with the electrons of the crystal materials (Guinier, 1994). The wave nature of the x-rays means that they are reflected by the lattice of the crystal, as shown in Figure 2.9 , to give a unique pattern of peaks of "reflections" at differing angles and of different intensity, just as light can be diffracted by a grating of suitably spaced lines. The diffracted beams from atoms in successive planes cancel unless they are in phase, and the condition for this is given by the Bragg relationship;

$$2dsin\theta = n\lambda \tag{2.1}$$

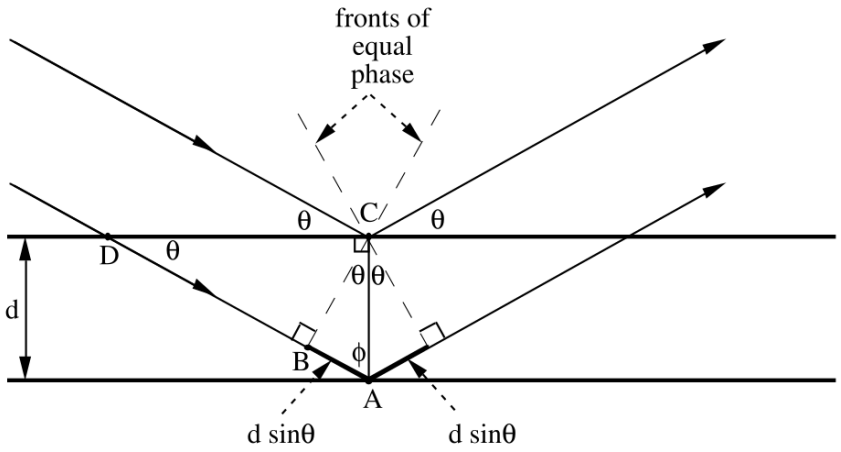

FIGURE 2.9 – Geometry for interference of a wave scattered from two planes separated by a spacing d.

where d is the distance between adjacent planes of atoms, θ is the angle of incidence of the x-ray beam, n is the order of the diffracted beam and λ represents the wavelength of the incident x-ray beam.

The Bragg condition can be satisfied for any set of planes whose spacing is greater than half the wavelength of the x-ray used (if d $< \lambda/2$, then $sin\theta > 1$, which is impossible). This condition sets a limit on how many orders of diffracted waves can be obtained from a given crystal using an x-ray beam of a given wavelength. Since the crystal pattern repeats in three dimensions, forming a three-dimensional diffraction grating, three integers, denoted (hkl) are required to describe the order of the diffracted waves. These three integers are defined as the Miller indices which used in crystallography, denote the orientation of the reflecting sheets with respect to the unit cell and the path difference in units of wavelength between identical reflecting sheets.

The Miller indices (hkl) can be calculated from Bragg's law:

$$2d_{hkl}sin\theta = n\lambda \tag{2.2}$$

In the cubic systems, the plane spacing is related to the lattice parameter and the Miller indices by the following relation:

$$d_{hkl} = \frac{a}{\sqrt{h^2 + k^2 + l^2}} \tag{2.3}$$

Combining equation (2.2) and (2.3), we get

$$a_{hkl} = \frac{n\lambda\sqrt{h^2 + k^2 + l^2}}{2sin\theta} \tag{2.4}$$

Considering the non cubic systems such as hexagonal system, the Miller indices can be calculated by using the lattice parameter from Bravais lattice:

$$\frac{1}{d_{hkl}^2} = \frac{4}{3}(\frac{h^2 + hk + k^2}{a^2}) + \frac{l^2}{c^2} \tag{2.5}$$

The information of an XRD pattern can be used to approximate the crystallite size of particles by using Debye-Scherrer formula (Warren, 1969):

$$D = \frac{K\lambda}{\beta cos\theta} \tag{2.6}$$

where D is crystalline size, λ is the wavelength of x-ray radiation (1.5418 Å for CuKα), β is the full wide at half maximum height (FWHM), K is the crystallite shape factor (usually taken as 0.9), θ is the diffraction angle.

2.3.1.1 Diffractometer of X-rays system:

X-ray diffraction spectrum is a recording of the diffracted intensity as a function of the angle 2θ formed with the incident beam. It makes it possible to obtain a great deal of many informationes especially on structural properties: crystallization (or not), presence of parasitic phase (s), crystallographic parameters, orientation and grain size (inversely proportional to the width at mid-height of the lines diffraction). [33]

The x-ray diffraction technique is normally carried out by an x-ray diffractometer. Essential components of a typical x-ray diffractometer used in a materials analysis laboratory include:

- A source of x-rays, usually a sealed x-ray tube,
- A "Goniometer" which provides precise mechanical motions of the tube, specimen, and detector,

- Electronics for counting detector pulses in synchronization with the positions of the goniometer
- An x-ray detector, the goniometer.

Typical data comprise a list of detector counts versus 2θ angle, whose graph is the diffraction pattern.

Our deposited undoped and Al doped ZnO thin films by spray pyrolysis were caracterized by X-ray diffraction (XRD) analysis using a PANalytical X'Pert Pro diffractometer from Mohamed Boudiaf M'sila University shown in figure 2.10 , using the k_α line of copper for a wavelength λ= 1.54060Å. The diffractograms were acquired in θ - 2θ geometry for an angular range of 20 to 70 °C.

2.3.2 Optical caracteristic:

The knowledge of optical constants of materials is frequently of great interest in the design and analysis of materials to be used in optoelectronics. Moreover, optical measurements are extensively used for characterization of composition and quality of the materials. It is possible to determine optical constants, such as refractive index, absorption coefficient, and dielectric constant by analyzing transmittance spectrum.

FIGURE 2.10 – Schematics of X ray equipement

Refractive index is one of the fundamental properties for an optical material, because it is closely related to the electronic polarizability of ions and the local field inside materials. The evaluation of refractive indices of optical materials is considerably important for the applications in integrated optic devices, such as switches, filters, and modulators. where refractive indices are the key constants for device design.

2.3.3 UV-visible spectroscopy

UV-Visible spectroscopy is a non-destructive technique and relies on the interaction of light with matter. A light beam of a certain wavelength range interacts with the sample and the intensity of the transmitted or reflected signal is recorded as a function of the wavelength. A diagram of the components of a typical spectrometer is shown in the Fig. 2.11.

A beam of light from a visible and/or UV light source is separated into its component wavelengths by a rotating prism or diffraction grating. The various wavelengths of a light source are separated and then selected by a slit such that a series of continuously increasing wavelengths pass through the slits for recording purpose. Each monochromatic beam in turn is split into two equal intensity beams by a half-mirrored

device. One of the beams, the sample beam, passes through the sample. The other beam, the reference, passes through an identical cuvette containing only the reference substrate. The intensities of these light beams are then measured by electronic detectors and compared. The intensity of the reference beam, which should have suffered little or no light absorption, is defined as I_0. The intensity of the sample beam is defined as I. If the sample compound does not absorb light of a given wavelength, I = I_0. However, if the sample compound absorbs light then I is less than I_0. This light absorption may be presented as

transmittance ($T_r = I/I_0$) or absorbance (A= log I_0/I). The absorption coefficient (α) can be calculated from the transmittance values in the transmittance spectra using the relation,

$$\alpha = -[log_e(1/T_r)/t] \tag{2.7}$$

Over a short period of time, the spectrometer automatically scans all the component wavelengths in the manner described. The ultraviolet (UV) region scanned is normally from 200 to 400 nm, and the visible portion is from 400 to 800 nm.

2.3.3.1 Device components:

The spectophotometer consists of the folowing elements:

- monochromatic light source
- monochromator(wavelength selection)
- tank
- detector

2.3.3.2 Device working principle:

UV-visible spectoscopy is carried out using a spectrophotometer. When the cell containing the solotion is placed in a spectroscope, it receives radiation of intensity I_0. Part of this incident light denoted I_0 is absorbed by the middle and the rest denoted I is transmitted.

The UV absorption edge is directly linked to the optical band gap. Indeed, the band gap can be estimated from the absorption edge by applying the Tauc relationship.The

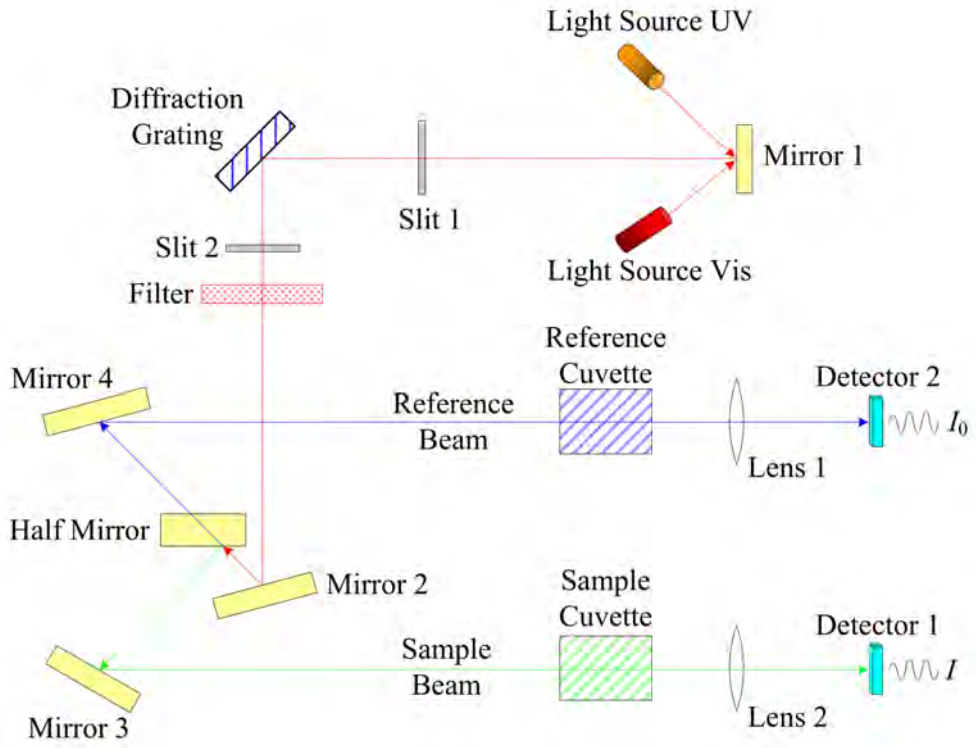

FIGURE 2.11 – Spectrophotometere uv-visible

variation of the absorption coefficient α in the strong absorption range is linked to the band gap Eg of the material by the following expression:

$$(\alpha hv) = A(hv - E_g)^n \tag{2.8}$$

Eg is the band gap energy and A is an energy-independent constant. The index n is characteristic of the nature of the optical absorption process.

Chapitre 3

Results and discussion

3.1 Structural characteristics

The X-ray diffraction is used to study the structural properties and the phase purity of the prepared thin films of ZnO and aliminium doped ZnO.

3.1.1 Spray pyrolysis Undoped ZnO thin films

Figure 3.1, illustrates the XRD pattern of the ZnO thin films deposited by spray pyrolysis method on the glass substrate at 450°C. The peaks of the XRD were observed between 2 θ = 20° and 70°.

Seven well-defined peaks are clearly observed in diffractogram at 2θ: 31.73°, 34.40°, 36.21°, 47.55°, 56.55°, 67,99°corresponding to (100), (002), (101), (102), (110), (103), (200) diffraction planes of ZnO, respectively. This results is in good agreement with PDF Code: 00-036-1451 and confirm the the polycrystalline wurtzite hexagonal structure of sprayed ZnO thin film.

No characteristic peaks were observed for other impurities. So, the XRD diffractogram revealed that wurtzite hexagonal ZnO thin film was successfully deposited by the spray pyrolysis technique. When compared the peaks, the intensity of the (002) peak is the most prominent, this indecate that the sprayed films show a preferred growth orientation along c-axis, which is perpendicular to the substrate. This preferred orientation is due to the minimal surface energy of the (0 0 2) plane that corresponds to the dense packed plane of the ZnO hexagonal structure [23].

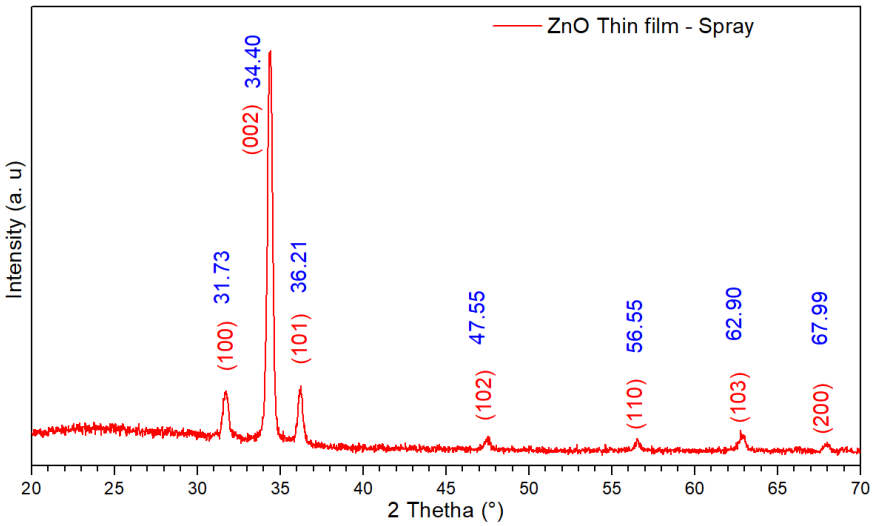

FIGURE 3.1 – Diffractograme of sprayed ZnO thin film.

As ZnO crystallizes in the wurtzite structure in which the oxygen atoms are arranged in a hexagonal close packed type with zinc atoms occupying half the tetrahedral sites. Zn and O atoms are tetrahedrally coordinated to each other and have, therefore, an equivalent position. The zinc structure is open with all the octahedral and half the tetrahedral sites empty. According to Bragg's law:

$$n\lambda = 2d_{hkl}sin\theta \tag{3.1}$$

where n is the order of diffraction (usually n = 1), k is the X-ray wavelength and d is the spacing between planes of given Miller indices h, k and l. In the ZnO hexagonal structure, the plane spacing d is related to the lattice constants a, c and the Miller indices by the following relation:

$$\frac{1}{d_{hkl}^2} = \frac{4}{3}(\frac{h^2 + hk + k^2}{a^2}) + \frac{l^2}{c^2} \tag{3.2}$$

With the first-order approximation, n = 1;

$$sin^2\theta = \frac{\lambda^2}{4a^2}[(h^2 + k^2 + hk) + l^2\frac{a^2}{c^2}] \tag{3.3}$$

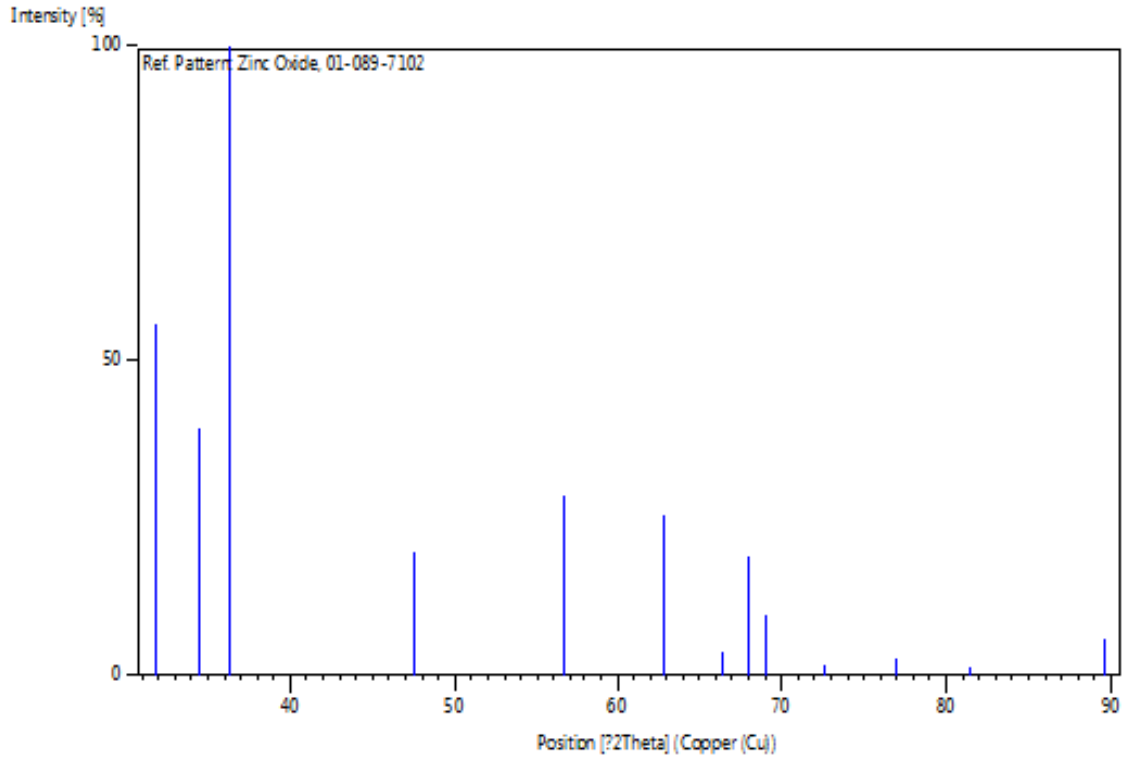

FIGURE 3.2 – Diffractograme of ZnO [01-070-2551].

The interplanar spacing ($d - hkl$) calculated from data XRD is compared with JCPDS data card and corresponding (hkl) planes and full width at half-maximum (FWHM) values for some major XRD peaks are summarized in Table 3.1.

Using the data obtained from XRD patterns to obtain detailed information about the structure properties of films such as crystalline size (D), lattice constants, dislocation density $<\delta>$ and macrostrain values are calculated.

- The average crystallite size of the deposited films has been calculated using the Scherrer's formula and Williamson Hall method:

$$D = \frac{K\lambda}{\beta cos\theta} \tag{3.4}$$

and Williamson Hall method equation:

TABLE 3.1 – XRD data and structural parameters of sprayed undoped ZnO thin film.

(hkl)	2θ (°)	2θ JCPDS	d XRD	d_0 JCPDS.
(100)	31.766	31,777	2,8169	2.8143
(002)	34.468	34,420	2.6020	2.6033
(101)	36.240	36,261	2.4788	2.4759
(102)	47.495	47,544	1.9143	1.9111
(110)	56.544	56,612	1.6276	1.6247
(103)	62.877	62,859	1.4780	1.4771
(200)	68.001	66,396	1.3786	1.4071

$$\frac{\beta.cos\theta}{\lambda} = \frac{k}{D_{w}} + \frac{\gamma sin\theta}{\lambda} \tag{3.5}$$

where D is the size of the crystallite, β is the full width at half maximum (FWHM) of the peak in radians and λ is the wavelength of the X-rays (1.5406 Å)

- The dislocation density σ can be found using the following formula expressed as the length of dislocation lines by unit volume of the crystal:

$$\delta = \frac{1}{D^2} \tag{3.6}$$

The expressions for lattice parameters (a and c) of the hexagonal ZnO lattice in the ZnO thin films was calculated using (100) and (002) diffraction peaks via :

the lattice constant "a" is calculated for (100) plane by using the expression 3.7 [35]:

$$a = \frac{\lambda}{\sqrt{3}.sin\theta} \tag{3.7}$$

The lattice constant "c" is calculated for (002) plane by using the expression 3.8 [35]:

$$c = \frac{\lambda}{sin\theta} \tag{3.8}$$

TABLE 3.2 – Lattice parameters, crystallize size (D), macro strain values (<e>) and dislocation density (δ) of sprayed undoped ZnO films.

	a(Å)	c(Å)	c/a	V(Å^3)	δ (10^{-3} nm^3)
Sprayed ZnO EXp. results	3.250	5.206	1,6018	47.62	53.2253
Ref. code N° 01-070-2551	3.249	5.207	1,6026	47.60	-

In thin films, strains originate mainly due to a mismatch between the polycrystalline film and the amorphous substrate and/or differences in coefficients of thermal expansion of the film and the substrate. The average uniform strain ϵ_z in the lattice along the c-axis in the randomly oriented ZnO films deposited on different substrate temperatures has been estimated from the lattice parameters using the following expression :

$$\epsilon_z = 100.\frac{c - c_0}{c_0} \tag{3.9}$$

where "c_0" is the lattice constant in unstrained ZnO it equal to c_0=0,5205 nm

The calculated lattice parameters along with their ratio 'c/a' are tabulated in Table

the internal relaxation parameter "u" for wurtzite structure is given by :

$$u = \frac{a^2}{3c^2} + 0.25 \tag{3.10}$$

Volume of ZnO unit cell 'V' is determined by using the expression :

$$V = \frac{\sqrt{3}a^2c}{2} \tag{3.11}$$

3.1.2 Spray pyrolysis of Aliminium doped ZnO thin films

Figure 3.3, illustrates the XRD pattern of the Al-doped ZnO thin film deposited by spray pyrolysis method on the glass substrate at 400°C. The peaks of the XRD were observed with 2θ from 20° to 70°.

Seven well-defined peaks are clearly observed in diffractogram at 2 θ 31.71°, 34.27°, 36.15°, 47.40°, 56.60°, 62,95°and 67,82 corresponding to (100), (002), (101), (102), (110), (103) and (200) respectively diffraction planes of ZnO doped, the results are indicating the polycrystalline wurzite structure of Al doped ZnO films. This study is in good agreement with PDF Code:01-070-2551 and confirm the wurtzite hexagonal structure of sprayed Al doped ZnO thin film. In addition the diffractogramme ao Al doped ZnO did not show any additional peaks, indicating that there are no new chemical phases.

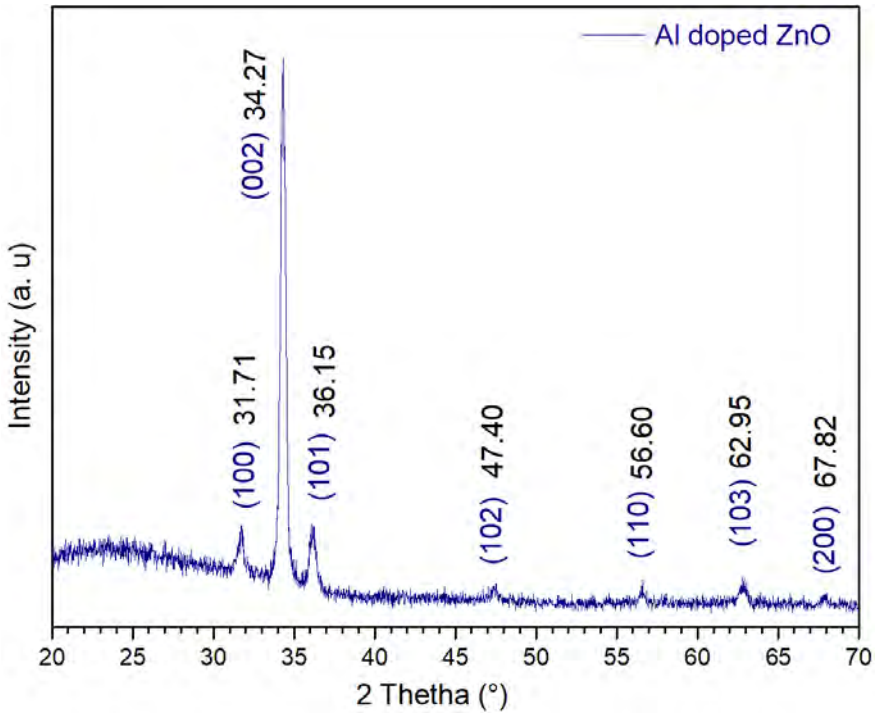

FIGURE 3.3 – Diffractograme of sprayed Al doped ZnO thin film.

We note that the doped samples have a good crystallynity. The lattice constants, crystallite size and dislocation density have been calculated from the 'd' values and these have been listed in table 3.3. The crystallite size and the apparent strain have been estimated by Scherrer equation

TABLE 3.3 – Interplanar spacing d_{hkl} from XRD, JCPDS data card for corresponding (hkl) planes, percentage of variation of d, and FWHM of Al doped ZnO sprayed films

(hkl) plane	2θ (°) Expt. results	2θ Ref. code N° 01-070-2551	d_{hkl} XRD	d_{hkl} Ref.
(100)	31.7176	31,777	2,8211	2.8143
(002)	34.2770	34,420	2.6161	2.6033
(101)	36.1563	36,261	2.4843	2.4759
(102)	47.4044	47,544	1.9178	1.911
(110)	56.6014	56,612	1.6261	1.6247
(103)	62.9534	62,859	1.4764	1.4771
(200)	68.8296	66,396	1.3817	1.4071

TABLE 3.4 – the lattice parameters

lattice	a(Å)	c(Å)	c/a	V(Å^3)
Sprayed ZnO EXp. results	3.254	5.227	1,6061	47.93
Ref. code N° 01-070-2551	3.249	5.207	1,6026	47.60

3.2 Optical properties

The UV-visible Spectro- photometer is used to study the optical properties and the transemittance of the thin films of ZnO and aliminium doped ZnO deposited by spry pyrolysis.

In order to correlate the optical behaviour of films with structural results, the optical transmittance of sample has been investigated in the wavelength range of 200–800 nm using UV–visible spectroscopy figure 3.4 It is clear that the sprayed ZnO thin films exhibit a high transmittance higher then 85 % in the visible region, It is clear observed a sharp absorption edges in the wavelength at approximately λ =372nm.

The optical transparency of AL doped ZnO sprayed thin films is typically investigated by direct measurements of the transmittance through the films on transparent substrates. However, GaAs is opaque in the visible wave- length range and transmittance measurements therefore cannot be applied in this case. The optical transmittance spectra of AL doped ZnO samples, in the wavelength range of 280 to 800 nm, are shown

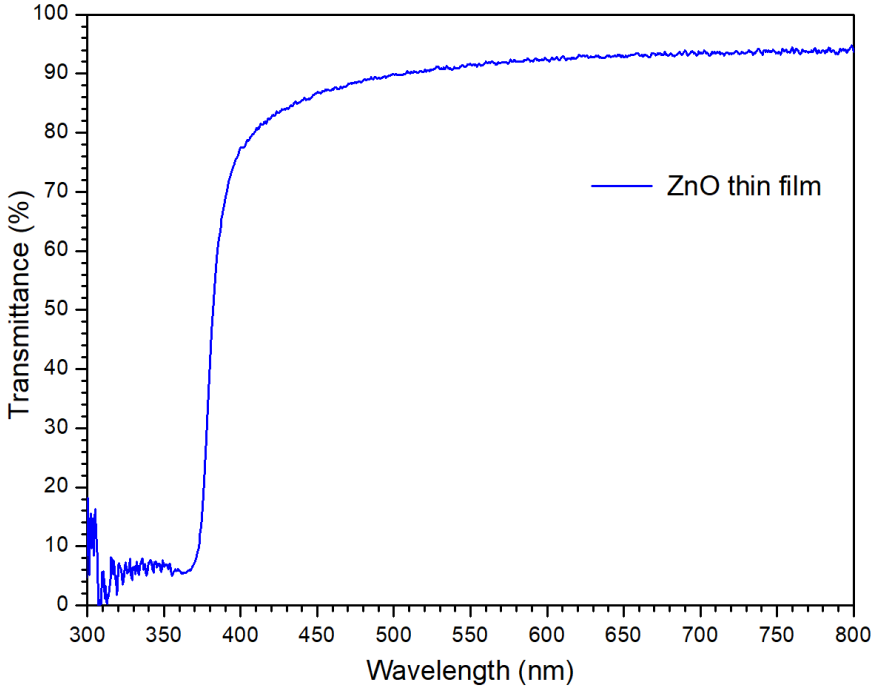

FIGURE 3.4 – Transmission spectra of sprayed ZnO thin film.

in figure3.5 . The interference fringes of the spectra for the films with deep valleys and tall crests indicate that the films have a smooth surface. In the visible range, the average optical transmittance is high, while the reflectance is low. In the near-IR range, the transmittance decreases while the reflectance starts increasing. It can be seen that the average transmittance in the visible wavelength region is about 90% for all the films with a sharp fundamental absorption edge.

For the undoped film, the transmittance is greater than 85% in the whole visible and near infrared .while the Al-doped film the transmittance is greater than 80% in the visible range. The films showed ultraviolet (UV) and defect related visible emissions in Fig.3.6 by FTIR spectrometer. In UV region, we can observe that the transmittance of ZnO Pure had started from 372 nm while Al doped ZnO started from 380 nm. A sharp increase in the transmittance indicating a direct transition in undoped ZnO with nonlinearity being observed in the high transparency in the visible region.In nother hand, Al doped ZnO thin films annealed at 400 °C had a slightly lower transmittance compared with undoped ZnO films in the visible region. The UV absorption edge

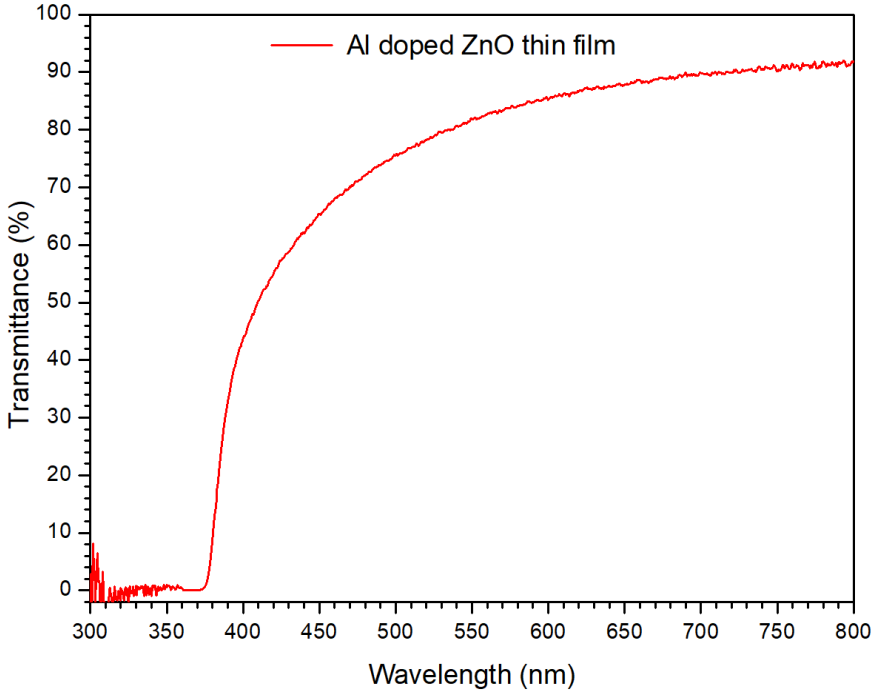

FIGURE 3.5 – Transmission spectra of sprayed ZnO thin film.

shifted towards a longer wavelength when it doped with Al. It observed that addition of Al to the starting solution increased the optical transmittance of the films.

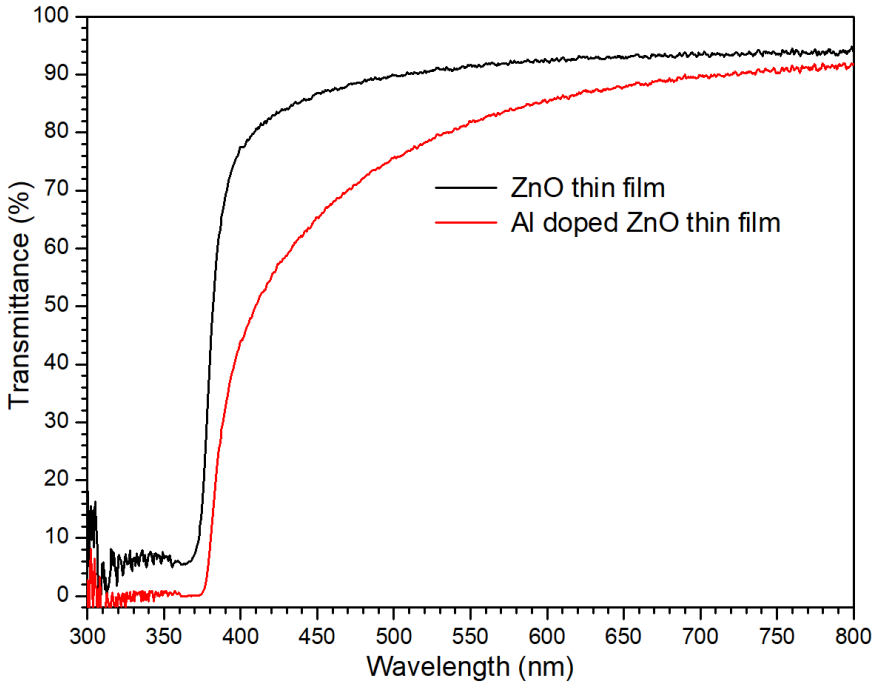

FIGURE 3.6 – Transmission spectra of sprayed doped and undoped ZnO thin film.

Conclusion

In this work of dessertation focuses on the deposition and properties study of zinc oxide thin films using the Spray pyrolysis technique from the solution prepared by chemical reaction between the precursors Zinc acetate dihydrate dissolved in the solvent (ethanol) and the stabilizer (monoethanolamine).
the deposited thin films have been characterized by X-ray diffraction (XRD) for structural properties study and UV-Visible spectroscopy for optical properties study.

- Structural characterization by the X-ray diffraction technique has shown that thin films are polycrystalline in a hexagonal würtzite structure, the calculation of the average crystallites size showed that they are of a nanometric order, i.e. 23 nm.

-The lattice parameters "a" and "c" and volume of unit cell in ZnO in good agreement with reference.

At the end of this study, we can say that Undoped and Al-doped ZnO thin films have been deposited onto glass substrates by the spray pyrolisis method and their structural and optical properties have been investigated. The XRD results showed that all films were crystallized under hexagonal wurtzite structure and presented a preferential orientation along the c-axis where the maximum crystallite size was found to be 25 nm for undoped film. The average transmittance of all films is over 80% in the visible region.

Bibliographie

[1] Srivastava, V., Gusain, D. and Sharma, Y. C. Synthesis, characterization and application of zinc oxide nanoparticles (n-ZnO). Ceram. Int. 39, 9803–9808 (2013). vi, 1, 4

[2] M.H.F. Sluiter, Y. Kawazoe, P. Sharma, A. Inoue, A.R. Raju, C. Rout, U.V. Waghmare, Phys. Rev. Lett. 94 (2005). p. 187204–1. 1

[3] Sagadevan, S., Vennila, S., Anita Lett, J., Marlinda, A. R., Aliya Binti Hamizi, N., and Rafie Johan, M. (2019). Tailoring the Structural, Morphology, Optical and Dielectric Characteristics of ZnO nanoparticles using Starch as a capping agent. Results in Physics, 102543. 1

[4] Sagheer, R. et al. Effect of Mg doping on structural, morphological, optical and thermal properties of ZnO nanoparticles. Optik (Stuttg). 200, (2020). 1

[5] Li, X. L. et al. Role of donor defects in enhancing ferromagnetism of Cu-doped ZnO films. J. Appl. Phys. 105, 1

[6] K. Raja, P. Ramesh, D. Geetha, Structural, FTIR and photoluminescence studies of Fe doped ZnO nanopowder by co-precipitation method, Spectrochim Acta Part A 131 (2014) 183–188. 1

[7] Ü. Özgür et al., "A comprehensive review of ZnO materials and devices," J. Appl. Phys., vol. 98, no. 4, pp. 1–103, 2005, doi: 10.1063/1.1992666. 2

[8] S. Hamrit, K. Djessas, N. Brihi, B. Viallet, K. Medjnoun, and S. E. Grillo, "The effect of thickness on the physico-chemical properties of nanostructured ZnO:Al TCO thin films deposited on flexible PEN substrates by RF-magnetron sputtering from a nanopowder target," Ceram. Int., 2016, doi: 10.1016/j.ceramint.2016.07.143. 2

[9] G. B. Murdoch, S. Hinds, E. H. Sargent, S. W. Tsang, L. Mordoukhovski, and Z. H. Lu, "Aluminum doped zinc oxide for organic photovoltaics," Appl. Phys. Lett., vol. 94, no. 21, pp. 21–24, 2009, doi: 10.1063/1.3142423. 2

[10] P. Saravanan, S. Alam, G.N. Mathur, Synthesis of ZnO and ZnS nano- crystals by thermal decomposition of zinc (II) cupferron complex, Mater. Lett. 58 (2004) 3528–3531. 2

[11] M.N. Kamalasanan, S. Chandra, Sol–gel synthesis of ZnO thin films, Thin Solid Films 288 (1996) 112–115. 2

[12] A. Boukhari et al., "Thickness effect on the properties of Mn-doped ZnO thin films synthesis by sol-gel and comparison to first-principles calculations," Ceram. Int., vol. 47, no. 12, pp. 17276–17285, 2021, doi: 10.1016/j.ceramint.2021.03.039. 2

[13] El Manouni et al., "Effect of aluminium doping on zinc oxide thin films grown by spray pyrolysis," Superlattices Microstruct., vol. 39, no. 1–4, pp. 185–192, 2006, doi: 10.1016/j.spmi.2005.08.041. 2

[14] J.E. Rodriguez, A.C. Caballero, Controlled precipitation methods: for- mation mechanism of ZnO nanoparticles, J. Eur. Ceram. Soc. 21 (2001) 925–930. 2

[15] B. Cheng, E.T. Samulski, Hydrothermal synthesis of one-dimensional ZnO nanostructures with different aspect ratios, Chem. Commun. (2004) 986–987. 2

[16] D.Y. Kim, S. Lee, Z.-H. Lin, K.H. Choi, S.G. Doo, H. Chang, J.-Y. Leem, Z.L. Wang, S.-O. Kim, High temperature processed ZnO nanorods using flexible and transparent mica substrates for dye-sensitized solar cells and piezoelectric nanogenerators, Nano Energy. 9 (2014) 101–111. 3

[17] S.-M. Lee, C. S. Choi, K. C. Choi, and H.-C. Lee, "Low resistive transparent and flexible ZnO/Ag/ZnO/Ag/WO3 electrode for organic light-emitting diodes," Org. Electron., vol. 13, no. 9, pp. 1654–1659, Sep. 2012, doi: 10.1016/j.orgel.2012.05.014. 3

[18] S. Abreu Fernandes et al., "Femtosecond Laser Ablation of ITO/ZnO for Thin Film Solar Cells," Phys. Procedia, vol. 41, no. 0, pp. 802–809, Jan. 2013, doi: 10.1016/j.phpro.2013.03.151. 3

[19] T. Chankhanittha and S. Nanan, "Visible-light-driven photocatalytic degradation of ofloxacin (OFL) antibiotic and Rhodamine B (RhB) dye by solvothermally grown ZnO/Bi2MoO6 heterojunction," J. Colloid Interface Sci., vol. 582, pp. 412–427, 2021, doi: 10.1016/j.jcis.2020.08.061. 3

[20] D.H. Ruddick, Zinc Oxide., 1984. 3

[21] Wahab, R., Hwang, H. Shin, H. Zinc Oxide Nanostructures and their Applications. 3

[22] Alias, S. S., Azmin, A. MoHamad. Synthesis of Zinc Oxide by Sol-gel-gel method for Phoeletrochemical Cells. 3

[23] Rebien, M., Henrion, W., Bär, M., Fischer, C.-H. (2002). Optical properties of ZnO thin films: Ion layer gas reaction compared to sputter deposition. Applied Physics Letters, 80(19), 3518–3520. 28

[24] Janotti, A., Van de Walle, C. G. (2005). Oxygen vacancies in ZnO. Applied Physics Letters, 87(12), 122102. doi:10.1063/1.2053360 6

[25] Handbook of Chemistry and Physics, 56th Edition, Ed. R.C. Weast, CRS Press, (1975) 6

[26] H.J. Lee, J.H. Kim, S.S. Park, S.S. H, G.D. Lee, Journal of Industrial and Engineering Chemistry 25 (2015) 199-206. 7

[27] A J Chen1,2, X M Wu1,2,3, Z D Sha1,2, L J Zhuge2,4 and Y D Meng3, Structure and photoluminescence properties of Fe-doped ZnO thin films https://doi.org/10.1016/j.apsusc.2009.12.035 ; Published 3 November 2006 7

[28] Ruddick, D. H. Zinc Oxide. Pigm for Pap (1984). doi:10.2165/00128415-200610940-00070. 8

[29] G.P. Dransfield, Radiat. Prot. Dosimetry 91, 271 (2000) 12. I. Perelshtein et al., Appl.Mat. Interfaces 1, 361 (2009) 13. S. Al-Hilli, M.Willander, Nanotechnology 20, 175103 (2009) 14. S. Al-Hilli et al., J. Appl. Phys. 102, 084304 (2007) 15. 8

[30] J.W. Kim et al., J. Nanoeng. Nanosystems, 2, 67 (2007) 9

[31] J.X.Wang et al., Appl. Phys. Lett. 88, 233106 (2006) 9

[32] A.F. Kohn, G. Ceder, D. Morgon, C. G. Van de Walle, Phys. Rev.B., 61 (2000) 15019. 22

[33] S. Suwanboon, Naresuan university journal.Vol. 16 (2) ,173- 180(2008) 24

[34] *Z.Q. Xu, H. Deng, Y. Li, Q.H. Guo, Y.R. Li*, Characteristics of Al-doped c-axis orientation ZnO thin films prepared by the sol–gel method, *Mater. Res. Bull.* 41 (2006) 354–358. 2

[35] P. Bindu, S. Thomas, Estimation of lattice strain in ZnO nanoparticles: X-ray peak profile analysis, *J. Theor. Appl. Phys.* 8 (2014) 123–134. 31

الملخص:

في هذا العمل، قمنا بتحضير ودراسة الخصائص البنيوية والخصائص الضوئية لرقائق أكسيد الزنك النقي ورقائق أكسيد الزنك المطعم بالألمنيوم، حيث قمنا بتحضير العينات بتقنية الرش الحراري على ركائز الزجاج عند درجة حرارة 400 درجة مئوية. الخصائص البنيوية تمت دراستها بواسطة جهاز حيود الأشعة السينية والخصائص الضوئية تمت دراستها بواسطة جهاز مطيافية الضوء المرئي والأشعة فوق البنفسجية. نتائج حيود الأشعة السينية أظهرت أن الرقائق لها بنية سداسية لأكسيد الزنك بتوجه مفضل على طول المحور C ولا يوجد أي طور آخر لمواد أخرى غير أكسيد الزنك. نتائج مطيافية الضوء المرئي وفوق البنفسجية تبين أن جميع رقائق أكسيد الزنك المحضرة شفافة في المجال المرئي وأن نسبة النفاذية أعلى من 85 ٪.

الكلمات المفتاحية

أكسيد الزنك، أكسيد الزنك المطعم بالألمنيوم، الأغشية الرقيقة، الرش الحراري، الخواص الضوئية، الخواص البنيوية.

Abstract

In the present work, undoped and Al doped ZnO thin films have been growth onto heated glass substrates at 400°C by Spray Pyrolysis technique. The structural and optical proprieties of sprayed thin films has been investigated. Structural analysis was carried out using X-ray diffraction. The optical properties were studied by mean of UV–visible spectrophotometry. The structural analysis indicates the presence of a single ZnO phase with a wurzite structure. The sprayed films show a preferred growth orientation along c-axis, which is perpendicular to the substrate. The optical transmittance spectra show a high transmission of films in the visible region.

Keywords: ZnO, Al doped ZnO, thin films, Spray Pyrolysis, structural proprieties, optical proprieties.

Résumé

Dans ce travail, nous avons étudié les propriétés structurales et optiques des couches minces de ZnO et des couches minces de ZnO dopé Al. Les couches minces ont été déposées par la méthode Spray Pyrolyse sur des substrats de verre à 400°C. Les résultats de diffraction des rayons X ont indiqué que les couches ont une structure hexagonale wurzite de ZnO sans aucune phase secondaire et avec une orientation préférentielle le long de l'axe C perpendiculaire à la surface du substrat. Les résultats de spectrophotométrie UV-visible ont montré que tous les films minces sont transparents avec une transmission moyenne supérieure à 85% dans le domaine de visible.

Mots clés : ZnO, ZnO dopé AL, couches minces, pyrolyse par pulvérisation, substrat de verre.